Influences of atmospheric turbulence effects on the orbital angular momentum spectra of vortex beams

Shiyao Fu and Chunqing Gao*

School of Opto-electronics, Beijing Institute of Technology, Beijing 100081, China
**Corresponding author: gao@bit.edu.cn*

Received April 12, 2016; revised June 3, 2016; accepted June 26, 2016;
posted June 27, 2016 (Doc. ID 262979); published July 29, 2016

We investigate the atmospheric turbulence effects on orbital angular momentum (OAM) spectra of different kinds of vortex beams, including Laguerre–Gaussian (LG) beams and Bessel beams, numerically. We generate the holograms of atmospheric turbulence with different structure constants of the refractive index. The OAM spectra of distorted single-mode or multiplexed LG beams and Bessel beams are analyzed. Compared with the OAM spectra of the two kinds of vortex beams, the spectrum of the Bessel beams is more dispersive. The results illustrate that Bessel beams suffer more from turbulent atmosphere than LG beams.

OCIS codes: (010.1330) Atmospheric turbulence; (050.4865) Optical vortices; (050.1940) Diffraction.
http://dx.doi.org/10.1364/PRJ.4.0000B1

1. INTRODUCTION

Vortex beams such as Laguerre–Gaussian (LG) beams and Bessel beams are intensively investigated for their unique performance. It was shown by Allen *et al.* that the complex amplitude of a vortex beam comprises an azimuthal phase term $\exp(il\phi)$, where ϕ is the azimuthal angle, and l is the topological charge [1]. And each photon in vortex beams carries the orbital angular momentum (OAM) of $l\hbar$ ($\hbar$ is Planck's constant divided by 2π).

There have been recent growing interest in applying vortex beams in free-space optical communications [2,3]. The topological charge l of a vortex beam, in principle, is an infinite integer value. In addition, the OAM of an optical beam can carry an unlimited number of bits. Therefore, vortex beams can tremendously increase the capacity of optical communication systems through mode multiplexing. Thus terabit free-space data transmission has been realized [2]. In general, LG beams are used as the vortex beams in free-space optical communication systems. However, another kind of vortex beam, the Bessel beam, also can be employed in the free-space multicasting [4]. Compared with LG beams, Bessel beams have the characteristics of nondiffraction [5], which means they are capable of recovering by themselves in the face of obstruction.

In a free-space optical communication system based on vortex beams, the effects caused by atmospheric turbulence should not be ignored. It is well known that the temperature and pressure's inhomogeneities of the atmosphere will contribute to the variations of the refractive index along the transmission path, which may distort the helical wavefront and increase the bit error rate (BER) of data transmission in optical communication systems [6]. The aberrant wavefront distorted by turbulence will also result in the OAM spectrum's dispersion [6,7]. The stronger the turbulence is, the more dispersive the spectrum will be. Hence, it is significant to evaluate the atmospheric turbulence effect on vortex beams by studying the variation of their OAM spectra.

Researchers have done a lot in assessing the atmospheric turbulence influence on vortex beams [6–10]. LG beams and Bessel beams can be utilized in high-capacity free-space data transmission through mode-division multiplexing. When they propagate through turbulent atmosphere simultaneously under the same condition (beam size, topological charge, turbulence strength, and so on), the influences of turbulent atmosphere on the OAM spectra of LG beams and Bessel beams have not been discussed simultaneously.

In this paper, we numerically study the variation of OAM spectrum when LG beams and Bessel beams propagate through atmospheric turbulence under the same condition in different cases. In addition, the case of transmission through the same turbulence strength at different propagation distances and the variation of the desired channel proportion of the two kinds of vortex beams are also investigated.

2. ATMOSPHERIC MODEL

To study the influence on vortex beams caused by turbulent atmosphere, the first thing to do is generate phase gratings that can simulate the turbulent atmosphere. The turbulence can be modeled by an Nth order matrix of random complex numbers with statistics that match Kolmogorov turbulence theory [11]. In our simulation, the turbulence model developed by von Karman is used [12,13]. It can be shown from modified von Karman spectrum, which includes the inner scale introduced by Tatarskii, that the spectrum of fluctuations in refractive index $\phi_n(\kappa)$ can be written as

$$\phi_n(\kappa) = 0.033C_n^2 \cdot (\kappa^2 + k_0^2)^{-11/6} \exp(-\kappa^2/k_m^2), \qquad (1)$$

where $k_0 = 2\pi/L_0$ and $k_m = 5.92/l_0$. Parameters L_0 and l_0 are the outer and inner scale of turbulence, respectively. In Eq. (1), κ denotes the spatial wavenumber, and C_n^2 is the structure constant of the refractive index, which represents the turbulence strength. Under the Markov approximation, the phase spectrum can be expressed as

$$\phi_\varphi(\kappa) = 2\pi k^2 z \phi_n(\kappa). \quad (2)$$

In Eq. (2), k denotes the wavenumber of the incident beam, and z can be regarded as the propagation distance in the turbulence. By this time, the phase distribution of turbulent atmosphere can be obtained according to Eq. (2) and [14] as

$$\varphi(x,y) = F\left[C \cdot \left(\frac{2\pi}{N\Delta x}\right) \cdot \sqrt{\phi_\varphi(\kappa)}\right], \quad (3)$$

where C is an $N \times N$ array of complex random numbers with zero mean and variance 1. Δx is the grid spacing and F denotes the Fourier transformation.

However, the approach shown above does not produce strict phase gratings because we cannot sample the spatial-frequency grid low enough to accurately represent low-order modes such as tilt. It was reported by Lane *et al.* that, by implementing the subharmonic method, can we acquire the accurate turbulent simulations [15]. The phase distribution of low spatial frequency by this method is a sum of M different screens, which is written as

$$\varphi_L(x,y) = \sum_{P=1}^{M} \sum_{n=-1}^{1} \sum_{m=-1}^{1} c_{n,m,P} \exp[i2\pi(f_{x_n}x + f_{y_m}y)], \quad (4)$$

where each value of the index P denotes a different grid, and the sums over n and m are over discrete frequencies. $c_{n,m,P}$ is the random draws of Fourier coefficients, and its derivation refers to [15]. f_{x_n} and f_{y_m} are the frequency grid. In our simulation, a 3×3 grid of frequencies is used for each value of P, and $M = 3$ different grids are used. Hence, the frequency grid spacing for each P is $1/(3^P D)$, where D is the screen's size. By this method, the original sample grid of spatial frequency is replaced by 3^{2P} small samples.

We do the simulation under three different turbulence strengths, the structure constant of the refractive index C_n^2 of which is 1×10^{-13}, 1×10^{-14}, and 1×10^{-15} $\mathrm{m}^{-2/3}$ separately. All of the basic parameters of these three phase screens are identical except the structure constant. In the process of generating the phase screen, the outer scale of the turbulence is 100 m, and the inner scale is 0.01 m. The wavelength of the incident beams is chosen as 1550 nm. The size of the screen is set as 0.44 m, and N is 1000. Notably, each propagation distance z is 100 m, and the simulations are repeated 10 times in order to compute the optical fields after propagating a distance of 1 km in turbulence.

3. SIMULATION

The single-mode or multiplexed LG beams and Bessel beams with the same topological charge are generated in our simulation. To compare the turbulence effect on these two kinds of vortex beams, the waist size of the inner ring of the Bessel beam is set the same as the LG beam.

We first investigate the difference of the turbulence effect on single-mode LG beams and Bessel beams under the same condition. In calculations, both of the two optical vortices carry the OAM of $3\hbar$, and the waist size is 0.06 m (for LG beams, the fundamental mode waist size $\omega_0 = 0.03$ m; for Bessel beams, the radial wave vector $k_r = 91.01$ m^{-1}). Figure 1 illustrates the intensity and the phase distribution before and after propagating through different atmospheric turbulence at the distance of 1 km. The optical fields after the turbulence are calculated through the scalar diffraction theory in our simulation. It is easy to find from Fig. 1 that, under the same condition, the stronger the turbulence is, the more distorted the beams will be. When $C_n^2 = 1 \times 10^{-13}$ $\mathrm{m}^{-2/3}$, the phases of the two vortex beams are totally chaotic.

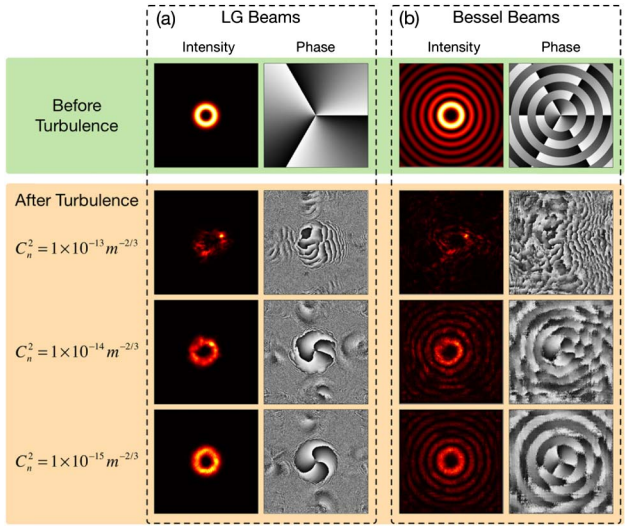

Fig. 1. Intensity and phase distribution before and after propagating through the atmospheric turbulence at the distance of 1 km with different C_n^2. (a) Case of LG beams. (b) Case of Bessel beams. In the map of the phase distribution, black denotes 0 and white denotes 2π.

In order to quantitatively study the effect of atmospheric turbulence on different kinds of optical vortices, we analyze the OAM spectrum before and after propagating through the atmospheric turbulence. The weight of each OAM channel can be obtained, if we project the coherent beam to a series of spiral harmonics in the form of $\exp(il\phi)$ and gain the relative power corresponding to all these harmonics [16]. Then the OAM spectrum that consists of the weight of power is acquired. The OAM spectra of single-mode LG beams and Bessel beams before and after turbulence are calculated and displayed in Fig. 2.

Under the strong turbulence ($C_n^2 = 1 \times 10^{-13}$ $\mathrm{m}^{-2/3}$), it can be seen from Fig. 2(b) that a large cross-talk arises for

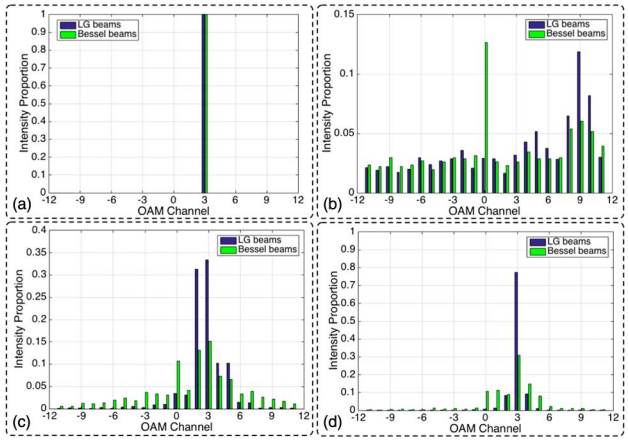

Fig. 2. OAM spectra of single-mode LG beam and Bessel beam with topological charge of +3 before and behind turbulence. (a) Case of before propagating through turbulence. (b), (c), and (d) Cases of after propagating through turbulence at the distance of 1 km and with C_n^2 of 1×10^{-13}, 1×10^{-14}, and 1×10^{-15} $\mathrm{m}^{-2/3}$, respectively.

the LG beams and the Bessel beams. We even cannot find how much OAM the incident beams carry. The OAM spectra shown in Figs. 2(c) and 2(d) illustrate that, in medium ($C_n^2 = 1 \times 10^{-14}$ m$^{-2/3}$) or weak ($C_n^2 = 1 \times 10^{-15}$ m$^{-2/3}$) turbulence, the spectrum of a single-mode Bessel beam is more dispersive than the LG beam, when they passed through the atmospheric turbulence with all the factors such as the turbulence strength, the beam size and so on are identical. It also means that the wavefront of the Bessel beam will suffer more than the LG beam in a turbulent atmosphere, resulting in the cross talk and bigger BER of a data transmission, although Bessel beams are free of obstructions.

Moreover, we study the difference of the turbulence effect on multiplexed vortex beams. Both of the multiplexed LG beams and multiplexed Bessel beams consist of four channels. The topological charges of the four channels are −6, −2, +3, and +7, respectively. And the intensity proportion of the four channels is identical. In addition, the fundamental waist size of each LG beam is 0.03 m, and the radial wave vector of the four Bessel beams are 112.54, 92.63, 91.01, and 118.94 m^{-1}, respectively, which makes the inner ring waist size of each channel of Bessel beams identical to the corresponding channel of LG beams, to create the same collating condition. The intensity and the phase profile of the two multiplexed vortex beams before and after propagating a distance of 1 km in different atmospheric turbulence are displayed in Fig. 3. The OAM spectra are shown in Fig. 4. The simulation results of multiplexed vortex beams are in agreement with the cases of single mode. It can be found from the OAM spectrum in Fig. 4 that the turbulence effect on the LG beams and Bessel beams is in relation to the turbulence strength. The OAM spectrum of Bessel beams is more dispersive, and the cross talk is more serious than LG beams. The desired channel proportion of Bessel beams is lower than LG beams even in weak turbulence ($C_n^2 = 1 \times 10^{-15}$ m$^{-2/3}$).

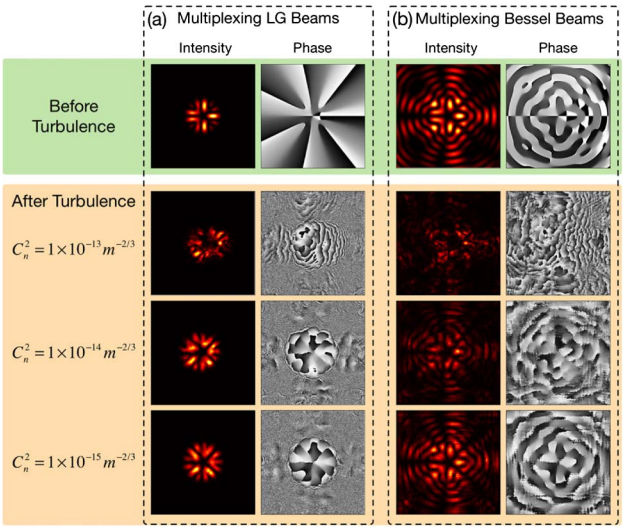

Fig. 3. Intensity and phase distribution of multiplexed vortex beams before and after propagating through the atmospheric turbulence at the distance of 1 km with different C_n^2. The multiplexed beams consist of four channels, whose topological charges are −6, −2, +3, and +7, respectively. (a) Case of multiplexed LG beams. (b) Case of multiplexed Bessel beams. In the map of the phase distribution, black denotes 0 and white denotes 2π.

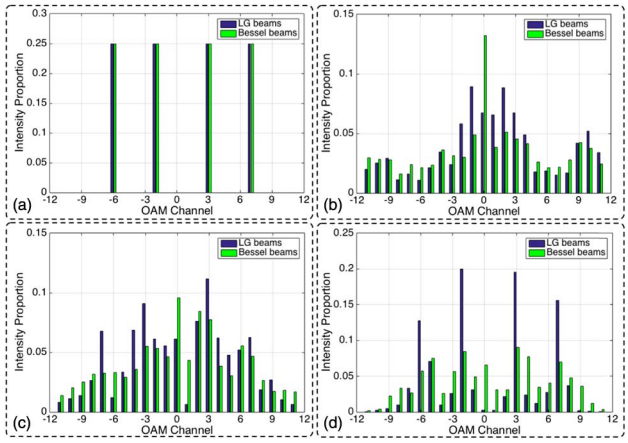

Fig. 4. OAM spectra of multiplexed LG beams and Bessel beams with topological charge of −6, −2, +3, and +7 before and behind turbulence. (a) Case of before propagating through turbulence. (b), (c), and (d) Cases of after propagating a distance of 1 km through turbulence with C_n^2 of 1×10^{-13}, 1×10^{-14}, and 1×10^{-15} m$^{-2/3}$, respectively.

4. DISCUSSION AND CONCLUSION

Under the same turbulence strength, the OAM spectra of beams that pass through the turbulence with different propagation distance are further investigated. We choose single-mode LG beams and Bessel beams with topological charge of +3 as the incident rays. The waist radii of the LG beams and the inner ring of Bessel beams are identical, the parameters of which are the same as the previous simulation of single mode. Ten phase screens of turbulence, whose C_n^2 is 1×10^{-14} m$^{-2/3}$ and propagation distance is 100 m, are used in the calculation to cover the varying propagation distance. The intensity proportion of the desired OAM channel ($l = +3$) is computed through analyzing the OAM spectrum. We figure out a group of proportions per 100 m and measure for 1 km. Then a curve to describe the relationship between the desired channel proportion of the two vortex beams and the propagating distance is obtained, which is depicted at Fig. 5(a).

It can be found from Fig. 5(a) that the curve of Bessel beams undulates stronger than that of LG beams. We compute the average and the variance of the two groups of channel proportions. As for LG beams, the average $\overline{x}_{\mathrm{LG}} = 0.8653$, the variance $\sigma_{\mathrm{LG}}^2 = 0.0186$. And for Bessel beams, the average $\overline{x}_{\mathrm{BS}} = 0.6049$, the variance $\sigma_{\mathrm{BS}}^2 = 0.0686$. The larger variance and the lower average of Bessel beams mean their wavefront distortion is more serious than LG beams when they pass through turbulent atmosphere with all the factors being identical.

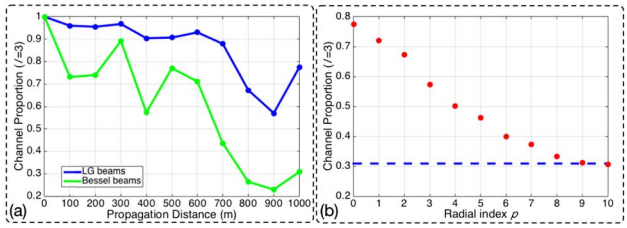

Fig. 5. (a) Curves show the relationship between the desired channel proportion of the two vortex beams and the propagating distance. (b) Desired channel proportions of LG beams with different radial index when they propagate through weak turbulence ($C_n^2 = 1 \times 10^{-15}$ m$^{-2/3}$) at the distance of 1 km.

Based on the OAM spectra discussed above, we can conclude that Bessel beams will suffer more than LG beams in passing through atmospheric turbulence under the same condition. It also can be understood with the help of Fried's parameter [17], which can be calculated from C_n^2 by the formula:

$$r_0 = (0.423k^2C_n^2z)^{-3/5}. \quad (5)$$

The turbulence strength is imposed on the beams, which can be characterized by d/r_0, with d being the beam diameter at the turbulence [6]. In each of our calculations, r_0 is a constant according to Eq. (5). Although the waist radii of the inner ring of Bessel beams we set is identical with the waist of LG beams, the side rings of Bessel beams enlarge the beam diameter indeed. Therefore, compared with LG beams, Bessel beams will suffer more from turbulent atmosphere.

We have analyzed the OAM spectra difference of LG beams and Bessel beams. While all of the above are the cases of single-ring LG beams (the radial index of LG beams $p = 0$). When $p \neq 0$, multiring LG beams will appear. Under the same topological charge and fundamental mode waist, the waist size of multiring LG beams can be expressed as $\sqrt{(2p + |l| + 1)/(|l| + 1)} \cdot \omega_l$, where ω_l are the waist size of single-ring LG beams. With the increasing of p, the optical fields will be more similar with those of Bessel beams. We also make a simulation to show the relationship between the desired channel proportion and the radial index of LG beams. The simulation is based on the work shown in Figs. 1 and 2. We do the simulation under weak turbulence ($C_n^2 = 1 \times 10^{-15}$ m$^{-2/3}$), and all the factors are the same as those in the previous single-mode simulation. The desired channel proportions of 11 different p are figured out, as shown in Fig. 5(b). In Fig. 5(b), the blue dashed line corresponds to the channel proportion of Bessel beams. And the red dots denote the measured proportion of LG beams with different radial index p. It is easy to find that the proportions are monotone decreasing as the increasing of p, and they will be very close to the dashed line.

The scatter diagram shown in Fig. 5(b) also can be understood by Eq. (5). We know the increasing of p will contribute to a larger beam diameter d. According to Eq. (4), larger d means larger influence. Hence the desired mode proportion will decrease.

One thing should be noticed is that our study is based on the assumption that the diameters of the Bessel beam's inner ring and LG beams are identical, resulting in the disagreement with some other work such as in [18]. In addition, a Bessel beam has infinitely extending sidelobes, which means it is not realistic. Hence, in the simulation, we clip the plane by a square for the initial plane of Bessel beams, leading to results that may depend on the size of the square considered to calculate. While in practical applications, the center part of Bessel beams is merely utilized. Therefore, our work is significant.

In brief, we have numerically demonstrated the atmospheric turbulence effects on different kinds of vortex beams, including LG beams and Bessel beams through analyzing their OAM spectra. The computed OAM spectra summarize that the cross talk of Bessel beams is larger, and the desired channel proportion is lower than LG beams. The simulation results mean Bessel beams suffer more from turbulence than LG beams under the same condition. We also explain the reason of the spectrum difference between Bessel beams and LG beams, which can be understood, as the side rings of Bessel beams enlarge the beam diameter.

Our work can be a reference for building a free-space optical data transmission link based on OAM. As for a short transmission distance, such as the system reported in [4], Bessel beams will be more dominant than LG beams because of their characteristic of being free from obstructions. But, for a long transmission distance without an adaptive optical system, the use of single-ring LG beams will be better.

Funding. National Basic Research Program of China (973 Program) (2014CB340004, 2014CB340002).

REFERENCES

1. L. Allen, M. W. Beijersbergen, R. J. C. Spreeuw, and J. P. Woerdman, "Orbital angular momentum of light and the transformation of Laguerre–Gaussian laser modes," Phys. Rev. A **45**, 8185–8189 (1992).
2. J. Wang, J. Y. Yang, I. M. Fazal, N. Ahmed, Y. Yan, H. Huang, Y. Ren, Y. Yue, S. Dolinar, M. Tur, and A. E. Willner, "Terabit free-space data transmission employing orbital angular momentum multiplexing," Nat. Photonics **6**, 488–496 (2012).
3. S. Yu, "Potentials and challenges of using orbital angular momentum communications in optical interconnects," Opt. Express **23**, 3075–3087 (2015).
4. L. Zhu and J. Wang, "Demonstration of obstruction-free data-carrying N-fold Bessel modes multicasting from a single Gaussian mode," Opt. Lett. **40**, 5463–5466 (2015).
5. J. Durnin, "Exact solutions for nondiffracting beams. I. The scalar theory," J. Opt. Soc. Am. A **4**, 651–654 (1987).
6. Y. Ren, H. Huang, G. Xie, N. Ahmed, Y. Yan, B. I. Erkmen, N. Chandrasekaran, M. P. J. Lavery, N. K. Steinhoff, M. Tur, S. Dolinar, M. Neifeld, M. J. Padgett, R. W. Boyd, J. H. Shapiro, and A. E. Willner, "Atmospheric turbulence effects on the performance of a free space optical link employing orbital angular momentum multiplexing," Opt. Lett. **38**, 4062–4065 (2013).
7. G. A. Tyler and R. W. Boyd, "Influence of atmospheric turbulence on the propagation of quantum states of light carrying orbital angular momentum," Opt. Lett. **34**, 142–144 (2009).
8. C. Paterson, "Atmospheric turbulence and orbital angular momentum of single photons for optical communication," Phys. Rev. Lett. **94**, 153901 (2005).
9. P. Birch, I. Ituen, R. Young, and C. Chatwin, "Long-distance Bessel beam propagation through Kolmogorov turbulence," J. Opt. Soc. Am. A **32**, 2066–2073 (2015).
10. K. Cheng, H. R. Zhang, and B. D. Lv, "Coherence vortex properties of partially coherent vortex beams," Acta Phys. Sin. **59**, 246–255 (2010).
11. T. S. McKechnie, *General Theory of Light Propagation and Imaging through the Atmosphere* (Springer, 2016).
12. T. V. Karman, "Progress in the statistical theory of turbulence," Proc. Natl. Acad. Sci. USA **34**, 530–539 (1948).
13. V. E. Ostashev, B. Brahler, V. Mellert, and G. H. Goedecke, "Coherence functions of plane and spherical waves in a turbulent medium with the von Karman spectrum of medium inhomogeneities," J. Acoust. Soc. Am. **104**, 727–737 (1998).
14. E. M. Johansson and D. T. Gavel, "Simulation of stellar speckle imaging," Proc. SPIE **2200**, 372–383 (1994).
15. R. G. Lane, A. Glindemann, and J. C. Dainty, "Simulation of a Kolmogorov phase screen," Waves Random Media **2**, 209–224 (2006).
16. Y. D. Liu, C. Gao, M. Gao, and F. Li, "Coherent-mode representation and orbital angular momentum spectrum of partially coherent beam," Opt. Commun. **281**, 1968–1975 (2008).
17. D. L. Fried, "Statistics of a geometric representation of wavefront distortion," J. Opt. Soc. Am. **55**, 1427–1435 (1965).
18. I. P. Lukin, "Variance of fluctuations of the orbital angular momentum of Bessel beam in turbulent atmosphere," Proc. SPIE **8696**, 869607 (2012).